Canadian Mineralogist
Vol. 24, pp. 625-642 (1986)

STRUCTURAL HIERARCHY IN $^{VI}M_x^{III}T_y\phi_z$ MINERALS

FRANK C. HAWTHORNE
Department of Geological Sciences, University of Manitoba, Winnipeg, Manitoba R3T 2N2

ABSTRACT

Based on the hypothesis that crystal structures may be ordered according to the polymerization of the co-ordination polyhedra with higher bond-valences, a hierarchical classification is set up for mineral structures that are based on triangular and octahedral cation co-ordination groups. It incorporates large sections of the carbonate, borate, selenite, tellurite, arsenite and antimonite chemical groups. The minerals are arranged according to their basic heteropolyhedral cluster, or fundamental building block (FBB), and the dimensional character of the cluster polymerization. The FBB, repeated by glide planes and screw axes, forms the structure module, a complex anionic polyhedral array whose excess charge is balanced by (extra-modular) large low-valence cations. The mode of polymerization of the FBB is related to the Lewis basicity of the simple oxyanions that constitute this FBB. The Lewis basicity of the structure module may be related, *via* the valence-matching principle, to the Lewis acidity of the extra-modular cations. With anion co-ordination numbers chosen so that they result in the most nearly equal bond-valences for the extra-modular cations, the co-ordination number (and Lewis acidity) of the extra-modular cation(s) can be predicted.

Keywords: structural classification, carbonates, borates, selenites, tellurites, arsenites, antimonites.

SOMMAIRE

Dans l'hypothèse que les structures cristallines peuvent être systématiquement ordonnées d'après la polymérisation des polyèdres de coordination à haute valeur de liaison, on établit une classification hiérarchique des structures de minéraux qui comportent des groupes de coordination cationiques triangulaires et octaédriques. Elle englobe, en grande partie, les carbonates, borates, sélénites, tellurites, arsenites et antimonites. Les minéraux y sont arrangés suivant leur groupement hétéropolyédrique, ou brique fondamentale (BF) et le nombre de dimensions des différents type de polymérisation. La BF, répétée par miroirs glisseurs ou axes hélicoïdaux, forme le module structural, polyèdre anionique complexe dont la charge résiduelle est neutralisée par les gros cations (hors-module) à valence basse. Le type de polarisation de la BF se relie à la basicité Lewis des oxyanions simples qui constituent cette BF. La basicité Lewis du module structural peut se relier, par simple neutralisation des charges, à l'acidité Lewis des cations hors-module. En choisissant les nombres de coordination de telle façon que les valences de liaison des cations hors-module soient le plus possible égales, on prédit et le nombre de coordination et l'acidité Lewis des cations hors-module.

(Traduit par la Rédaction)

Mots-clés: classification structurale, carbonates, borates, sélénites, arsenites, antimonites.

INTRODUCTION

There have been many suggestions that minerals should be classified according to their crystal structures, based on the idea that structure should be a more fundamental characteristic of a mineral than chemical composition. Many physical and chemical properties of a mineral can be rationalized in terms of atomic arrangement, and with the rapid increase in the number of mineral structures known, connections between structure and paragenesis are becoming apparent. Thus an adequate structural classification of minerals should provide an epistemological basis for the interpretation of the role of minerals in geological processes. A hierarchical scheme of this sort should apply to all minerals, and the physical, chemical and paragenetic characteristics of a mineral should be seen to arise as natural results of its crystal structure, and the interaction of that structure with the environment in which it occurs. Such a complete classification is still to be realized, but general structural schemes are now beginning to appear (Lima-de-Faria 1983, Hawthorne 1985a). They are based on the general idea of *modular crystallography,* whereby structures are categorized according to the character and polymerization of their basic structural units, or *fundamental building blocks.*

Hawthorne (1983) has proposed the following hypothesis: *structures may be ordered or classified according to the polymerization of those cation co-ordination polyhedra with higher bond-valences.* Hawthorne (1985a) showed how this hypothesis is suggested by Pauling's (1960) second rule and used it to develop a hierarchical classification and description of minerals of stoichiometry $MT_2\phi_n$ based on tetrahedrally and octahedrally co-ordinated cations. Hawthorne (in prep.) has extended this to all other minerals structurally based on octahedra and tetrahedra.

The fundamental ideas behind this approach are not restricted to any number or type of co-ordination polyhedra, and here I would like to examine all (or most) minerals based on triangular and octahedral co-ordinations; this encompasses minerals that are chemically classified as carbonates, borates, selenites, tellurites, arsenites and antimonites.

TABLE 1. $^{VI}M_x^{III}T_y\phi_z$ MINERALS BASED ON FINITE $[^{VI}M_x(T\phi_3)_y\phi_n]$ CLUSTERS

Mineral	Formula	a(Å)	b(Å)	c(Å)	β(°)	Sp.Gr.	Ref.
Baylissite	$K_2[Mg(CO_3)_2(H_2O)_4]$	11.404(4)	6.228(2)	6.826(2)	99.66(2)	P2₁/n	(1)

References: (1) Bucat et al. (1977)

PRELIMINARY CONSIDERATIONS

In addition to the hypothesis stated above, Hawthorne (1985a) has made some specific observations that pertain to the application of modular crystallography to the classification and description of crystal structures. Higher bond-valence polyhedra bond together to form *homo-* or *heteropolyhedral clusters* that constitute the *fundamental building block* (FBB) of the structure. The FBB is repeated, often polymerized, by translational symmetry operators to form the *structure module,* a complex anionic polyhedral array (not necessarily connected) whose excess charge is balanced by the presence of large low-valence cations. The possible modes of cluster polymerization result in the following possible types of structure module: (i) unconnected polyhedra, (ii) isolated (finite) clusters, (iii) infinite chains, (iv) infinite sheets and (v) infinite frameworks.

This paper will consider the $^{VI}M_x^{III}T_y\phi_z$ minerals (^{VI}M = [6]-co-ordinated cation, ^{III}T = [3]-co-ordinated cation, ϕ = unspecified ligand). In many cases, it is more instructive to write this formula as $M_x(T\phi_3)_y\phi_n$, where $n = z-3y$, as this carries more structural information. It should be emphasized that this formula is not necessarily the total formula of the mineral, but just the formula of that part that involves the (more strongly bonded) triangularly and octahedrally co-ordinated cations and their ligands.

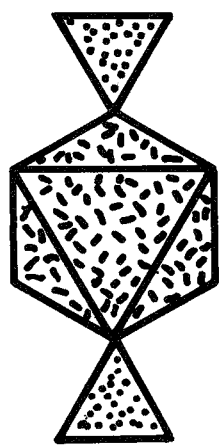

FIG. 1. The $[M(T\phi_3)\phi_4]$ finite cluster that is the FBB of the structure of baylissite.

STRUCTURAL CLASSES

Isolated polyhedra

There are no minerals in this particular class. This is a significant observation, as it suggests the question 'why are there no minerals of this particular type?'. This will be considered later, although it should be noted that synthetic inorganic solids do show this type of structural arrangement, *e.g.*, $Mn(NO_3)\cdot 6H_2O$ (Ribár *et al.* 1976) and $Fe(NO_3)\cdot 9H_2O$ (Hair & Beattie 1977).

Finite clusters

Baylissite (Table 1) is the one mineral based on finite clusters. The fundamental building block is the heteropolyhedral cluster $[Mg(CO_3)_2(H_2O)_4]$, in which the (CO_3) triangles are in a *trans* configuration with regard to the central octahedron (Fig. 1). These are repeated by the translational operators of the structure to form rather open sheets of finite clusters. Note the structural and paragenetic similarities with the analogous $^{VI}M^{IV}T_2\phi_n$ minerals anapaite, bloedite, leonite and schertelite (Hawthorne 1985a,c).

Infinite chains

Of the large number of possible infinite chains of the form $[^{VI}M_x(T\phi_3)_y\phi_n]$ that can be built from simple heteropolyhedral clusters of octahedra and triangles, only a very few types are actually found in minerals; these are schematically illustrated in Figure 2.

The $[M(T\phi_3)\phi_2]$ chain is the basis of the minerals of the dundasite group, hydrodresserite and dawsonite; in all of these minerals, the chain has the composition $[Al(CO_3)(OH)_2]$ with a repeat distance of approximately 5.6 Å. The octahedra share *trans* edges along the chain, and the triangles bridge adjacent vertices in a staggered fashion along the length of the chain; note the similarity to the analogous $[M(TO_4)\phi_2]$ chain found in the descloizite and conichalcite groups of minerals (Hawthorne, in prep.). In the dundasite group of minerals, the chains are linked by [9]-co-ordinated Pb, Ba or Sr, and hydrogen bonds involving (H_2O) groups that are not bonded to any cation (Fig. 3a). In hydrodresserite, the chains are linked by [9]-co-ordinated Ba

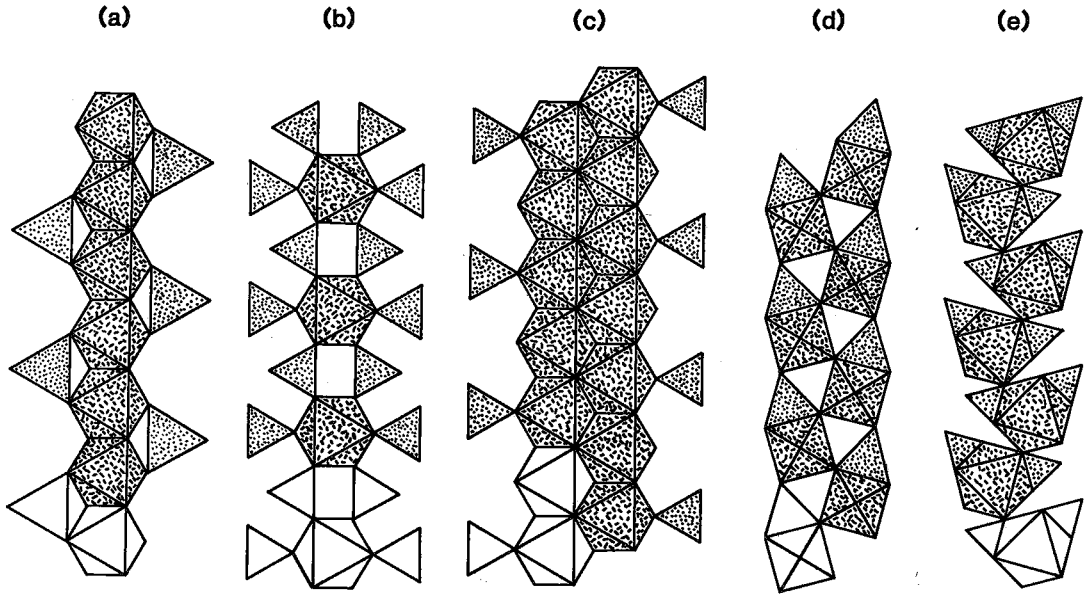

FIG. 2. Infinite $[M_x(T\phi_3)_y\phi_n]$ chains found in minerals: (a) $[M(T\phi_3)\phi_2]$, dundasite type; (b) $[M(T\phi_3)_4]$, sahamalite type; (c) $[M_2(T\phi_3)\phi_5]$, artinite type; (d) $[M(T\phi_3)\phi_2]$, nesquehonite type; (e) $[M(T\phi_3)\phi]$, chalconatronite type. The FBB of each chain is shown unshaded.

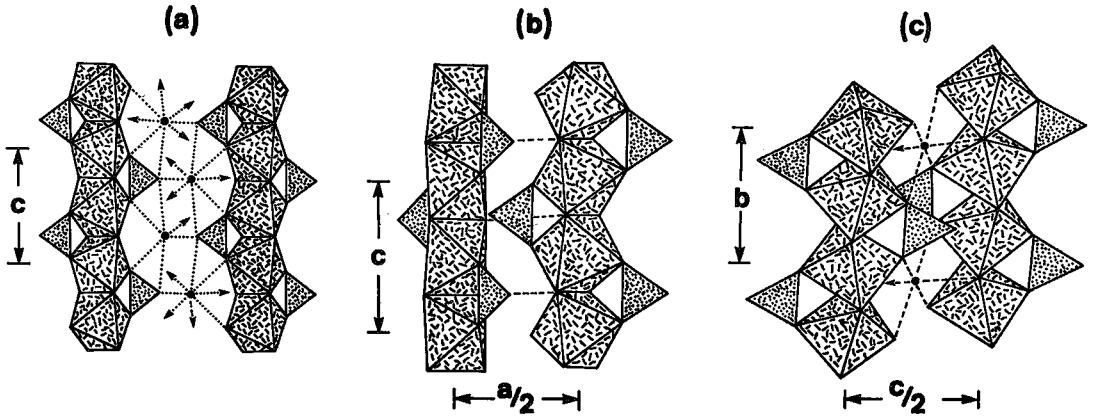

FIG. 3. The structures of minerals based on the $[M(T\phi_3)\phi_2]$ dundasite-type chain: (a) the structure of dundasite, projected down [110]; extra-modular Pb cations (black circles) link the $[Al(CO_3)(OH)_2]$ chains together; (b) the structure of hydrodresserite, projected down [010]; the $[Al(CO_3)(OH)_2]$ chains are linked by extra-modular Ba (not shown) and hydrogen bonds (some of which are shown as broken lines); (c) the structure of dawsonite, projected onto (011); the $[Al(CO_3)(OH)_2]$ chains are linked by extra-modular Na.

and a network of hydrogen bonds involving three non-modular (H_2O) groups; only one of the (H_2O) groups is bonded to Ba, and the others participate solely in the hydrogen-bonding network (Fig. 3b). In dawsonite, the $[Al(CO_3)(OH)_2]$ chains run parallel to [010], and are cross-linked by octahedrally co-ordinated Na and hydrogen-bonding involving the module (OH) ligands (Fig. 3c).

The least-connected chain is the $[M(T\phi_3)_4]$ chain (Fig. 2b) that is the basis of the structure of sahamalite (Table 2). In this mineral, $[(Mg,Fe^{2+})(CO_3)_4]$ chains run parallel to [001], with a repeat distance of approximately 4.6 Å, and are cross-linked by [9]-co-ordinated rare-earth cations (Fig. 4).

The $[M_2(T\phi_3)\phi_5]$ chain (Fig. 2c) is the basis of the structure of artinite (Table 2), in which an edge-

TABLE 2. $^{VI}M_x^{III}T_y\emptyset_z$ MINERALS BASED ON INFINITE $[^{VI}M_x(T\emptyset_3)_y\emptyset_n]$ CHAINS

Mineral	Formula	a(Å)	b(Å)	c(Å)	β(°)	Sp.Gr.	Ref.
Sahamalite	$(RE)_2[(Mg,Fe)(CO_3)_4]$	5.894(1)	16.116(3)	4.612(1)	106.54(1)	$P2_1/a$	(1)
Dresserite	$Ba[Al(CO_3)(OH)_2]_2(H_2O)$	9.27	16.8	5.63	-	Pbnm	-
*Dundasite	$Pb[Al(CO_3)(OH)_2]_2(H_2O)$	9.08(1)	16.37(2)	5.62(1)	-	Pbnm	(2)
Strontiodresserite	$(Sr,Ca)[Al(CO_3)(OH)_2]_2(H_2O)$	9.14(1)	15.91(1)	5.594(5)	-	Pbnm	-
Hydrodresserite†	$Ba[Al(CO_3)(OH)_2]_2(H_2O)_3$	9.755(1)	10.407(1)	5.632(1)	92.27(1)	$P\bar{1}$	(3)
Dawsonite	$Na[Al(CO_3)(OH)_2]$	6.759(1)	5.585(1)	10.425(1)	-	Imma	(4)
Artinite	$[Mg_2(CO_3)(OH)_2(H_2O)_3]$	16.560(5)	3.153(1)	6.231(3)	99.10(4)	C2/m	(5)
Nesquehonite	$[Mg(CO_3)(H_2O)_2]\cdot H_2O$	7.705(1)	5.367(1)	12.121(1)	90.45(1)	$P2_1/n$	(6)
Chalconatronite	$Na_2[Cu(CO_3)_2(H_2O)](H_2O)_3$	9.696(2)	6.101(2)	13.779(3)	91.83(2)	$P2_1/n$	(7)

References: (1) Pertlik & Preisinger (1983); (2) Cocco et al. (1972); (3) Szymański (1982); (4) Corazza et al. (1977); (5) Akao & Iwai (1977); (6) Stephan & MacGillavry (1972); (7) Mosset et al. (1978).
†α = 95.70(1)°, γ = 115.64(1)°. *indicates the principal mineral of the group.

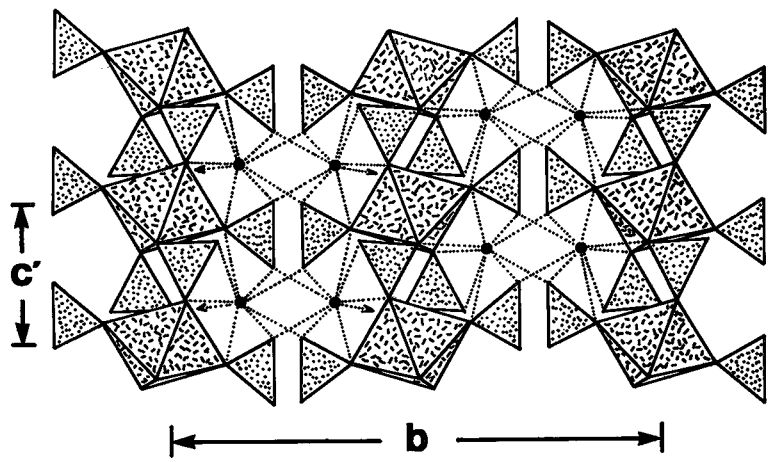

FIG. 4. The structure of sahamalite projected down [100]; the $[Mg,Fe^{2+})(CO_3)_4]$ chains are cross-linked by extra-modular [9]-co-ordinated *REE* cations (shown as black circles).

sharing ribbon of ($Mg\phi_6$) octahedra with corner-sharing (CO_3) groups extends along [010]. In the idealized chain of Figure 2c, there is an alternation of (CO_3) groups and (H_2O) groups along the edges of the octahedral ribbon, giving a chain-repeat distance of about 6.3 Å. In the artinite structure, adjacent chains have two possible relative positions, differing by a displacement of half the chain-repeat distance, and the chains are disordered over these two positions. This leads to a halving of the cell dimension in the direction of the chain (*i.e.*, along [010]) and diffuse layer-lines with $k = 2n+1$. Chains are linked by direct hydrogen-bonding from the (H_2O) groups of one chain to the oxygen atoms of the (CO_3) groups in adjacent chains.

Both nesquehonite and chalconatronite are characterized by fundamental building blocks in which there is edge-sharing between ($M\phi_6$) octahedra and ($T\phi_3$) triangles. In nesquehonite, the structure module is an array of heteropolyhedral chains of the form

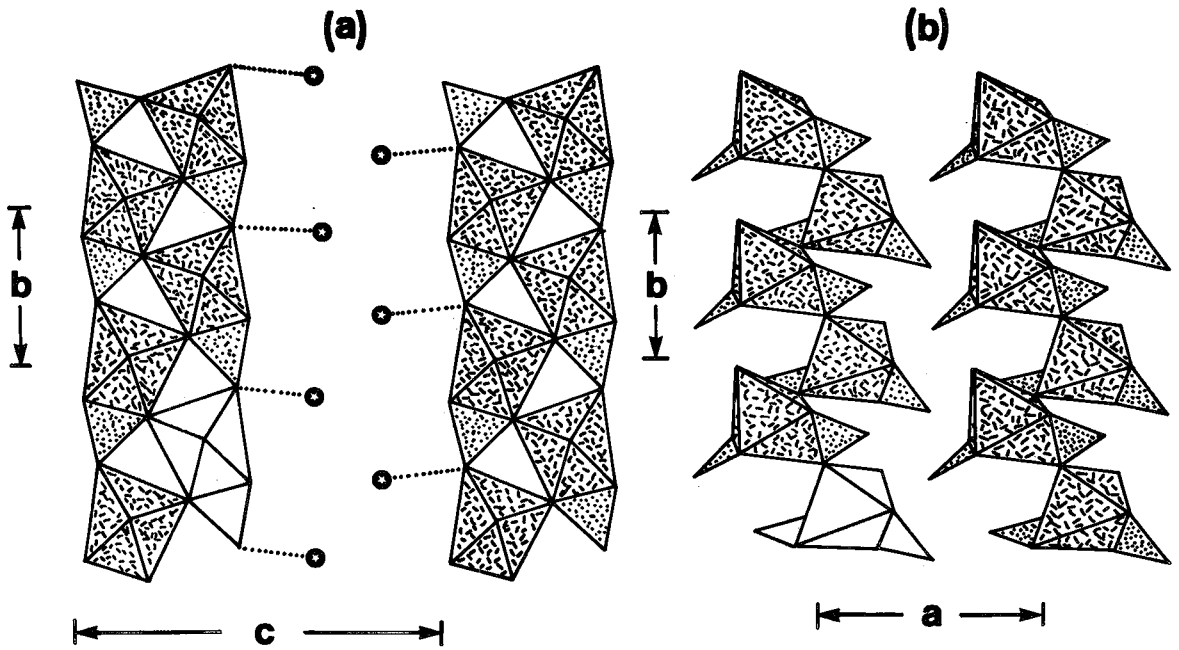

FIG. 5. The structures of (a) nesquehonite, projected onto (011); $[Mg(CO_3)(H_2O)_2]$ chains are linked by hydrogen-bonding, and the nonmodular (H_2O) group is shown by the star; chains underlie the nonmodular (H_2O) groups that link the chains *via* hydrogen bonds; (b) chalconatronite, projected down [001]; extra-modular Na (omitted for clarity) bonds the $[Cu(CO_3)_2(H_2O)]$ chains together.

TABLE 3. $^{VI}M_x{}^{III}T_y\emptyset_z$ MINERALS BASED ON INFINITE $[^{VI}M_x(T\emptyset_3)_y\emptyset_n]$ SHEETS

Mineral	Formula	a(Å)	b(Å)	c(Å)	Sp.Gr.	Ref.
Buetschliite	$K_2[Ca(CO_3)_2]$	5.38	a	18.12	$R\bar{3}2/m(?)$	(1)
*Eitelite	$Na_2[Mg(CO_3)_2]$	4.942(2)	a	16.406(7)	$R\bar{3}$	(2)
Tunisite	$NaCa_2Cl[Al_2(CO_3)_2(OH)_4]_2$	11.198(1)	a	6.564(1)	P4/nmm	(3)
Rodalquilarite†	$H_3Cl[Fe_2^{3+}(TeO_3)_4]$	8.89	5.08	6.63	$P\bar{1}$	(4)
Denningite	$(Ca,Mn)[(Mn,Zn)(Te_2O_5)_2]$	8.82(5)	a	13.04(5)	$P4_2/n$	(5)

References: (1) Pabst (1974); (2) Pabst (1973); (3) Effenberger et al. (1981); (4) Dusausoy & Protas (1969); (5) Walitzi (1965).

† $\alpha = 103.2$, $\beta = 107.1$, $\gamma = 77.9^0$

$[M(T\phi_3)\phi_2]$. An edge-sharing $[Mg(CO_3)O_2(H_2O)_2]$ cluster links by corner-sharing between a triangle and an octahedron, and between octahedra, to form the $[Mg(CO_3)(H_2O)_2]$ chain that extends along [010] with a repeat distance of around 5.4 Å. The chains are linked by a network of hydrogen bonds that involves both direct linkage between chains, and linkage through the third (H_2O) group that does not bond to any module cation but is only held in the crystal by the hydrogen-bond network (Fig. 5a). In chalconatronite, the fundamental building block is the edge-sharing $[M(T\phi_3)_2\phi_2]$ cluster that polymerizes by corner-sharing between a triangle and an octahedron, and between octahedra, to form an $[M(T\phi_3)_2\phi]$ chain of composition $[Cu(CO_3)_2(H_2O)]$. The original description of the structure assigned a co-ordination number of [5] to Cu, but bond-valence considerations show that the sixth distance of 2.597 Å should be considered. Adjacent chains are linked by [6]-co-ordinated Na and hydrogen bonds both from module (H_2O) and non-module (H_2O) groups that form part of the co-

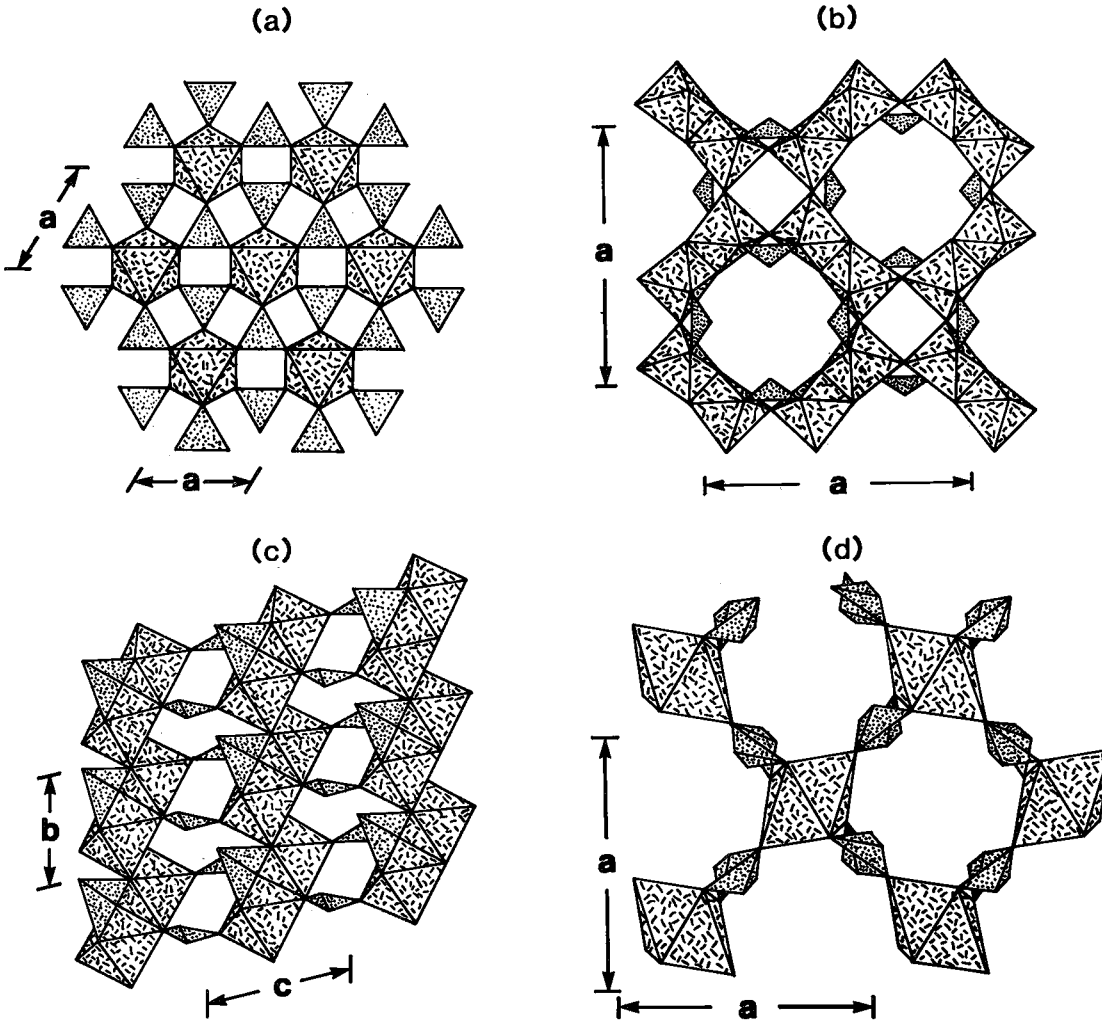

FIG. 6. Infinite-sheet modules found in minerals: (a) $[M(T\phi_3)_2]$, eitelite type; (b) $[M(T\phi_3)\phi_2]$, tunisite type; (c) $[M_2(T\phi_3)\phi_4]$, rodalquilarite type; (d) $[M(T_2\phi_5)_2]$, denningite type.

ordination polyhedra of the Na cations (Fig. 5b).

Infinite sheets

The minerals based on infinite sheets are listed in Table 3, and the sheet modules are illustrated in Figure 6.

The $[M(T\phi_3)_2]$ sheet, which is the basis of the eitelite group of structures, consists of corner-sharing triangles and octahedra extending parallel to (001) (Fig. 6a). Adjacent sheets are linked along [001] by [9]-co-ordinated alkali cations. The arrangement of the sheet module resembles that in the analogous $[M(T\phi_4)_2]$ minerals merwinite and brianite (Hawthorne 1985a).

Tunisite is based on a very elegant sheet of the type $[M(T\phi_3)\phi_2]$, involving corner-sharing between triangles and octahedra, and both corner- and edge-sharing between octahedra. The resulting arrangement is very open (Fig. 6b), and adjacent sheets are linked by [10]-co-ordinated Ca and [5]-co-ordinated Na.

The $[M_2(T\phi_3)_4]$ sheet illustrated in Figure 6c is found in the structure of rodalquilarite (Table 3). Serrated chains of edge-sharing (FeO_6) octahedra extend along [010], and these are cross-linked by (TeO_3) groups to form a sheet parallel to (100). The sheets are linked by a network of hydrogen bonds involving also the Cl anion. The details of the hydrogen positions are not known, but some strong near-

symmetrical hydrogen bonds are possible in this structure.

The last mineral in this class is denningite (Table 3), in which $[M(T_2\phi_5)_2]$ sheets are formed from corner-sharing between triangles (to form $(T_2\phi_5)$ dimers) and corner-sharing between these dimers and octahedra (Fig. 6d). These sheets are parallel to (001) in denningite and are cross-linked by [8]-co-ordinated Ca and Mn. Intersheet bonding is also quite strong, and thus denningite has strong affinities to framework structures.

Infinite frameworks

The minerals of this class are listed in Table 4, more or less in increasing order of connectivity of the structure module. First are the minerals of the calcite and dolomite groups; the structures are based on a framework of corner-sharing triangles and octahedra, and are not illustrated here. The minerals of the kotoite group are based on an $[M_3(T\phi_3)_2]$ framework involving edge- and corner-sharing between triangles and octahedra, and edge- and corner-sharing between octahedra (Figs. 7a,b). Viewed down [001], the structure shows striking similarities to that of lindgrenite $Cu_3(MoO_4)_2(OH)_2$ (Hawthorne & Eby 1985), with (BO_3) triangles in place of the (MoO_4) tetrahedra.

Huntite is based on an $[M_3(T\phi_3)_4]$ framework (Fig. 8) consisting of corner-linkage between (CO_3) triangles and (MgO_6) octahedra, and edge-sharing between (MgO_6) octahedra. From a bond-valence viewpoint, the Ca should also be included in the structure module, as it is also [6]-co-ordinated, but the co-ordination polyhedron is trigonal prismatic rather than octahedral.

The following minerals fall into a subgroup of the framework class, as they have strong structural affinities: fluoborite, painite, jeremejevite, warwickite, the ludwigite group of minerals, pinakiolite, orthopinakiolite, takeuchiite, wightmanite and the szaibelyite group of minerals. A prominent feature in the structures of all these minerals is the chain of edge-sharing octahedra (of the rutile type) with a repeat distance that is an integral multiple of 3 Å. These chains are cross-linked by $(T\phi_3)$ triangles in the plane perpendicular to the length of the chains, and by sharing edges and vertices with adjacent chains. Ignoring ordering along the length of the chains, the graphical aspects of these structures may be idealized as colorings on the regular 3^6 net; because of this 2-dimensional character to these structures, Moore & Araki (1974) referred to them as the "3 Å wallpaper structures". The idealized frameworks, projected down the $3n$ Å axis and mapped on to the 3^6 net, are shown in Figure 9. The simplest structure is that of fluoborite (Fig. 9a), in which the octahedral chains occur in pairs, and by sharing vertices form a triangular tunnel across which the (BO_3) groups bond; note the similarity of the projection of this chain to the Keggin molecule, with the triangle replacing the tetrahedron, a complex heteropolyhedral cluster commonly found in $M_x(TO_4)_y\phi_n$ structures (Moore & Araki 1977). Moore & Araki (1976) drew attention to the large pipe-like hexagonal channel running through the origin (Fig. 9a); in fluoborite, this channel is empty. The structure of painite (Table 4) is very similar to that of fluoborite, albeit the chemistries of the structures are radically different. In painite, the octahedra have the same arrangement as in fluoborite, but are occupied by Al rather than Mg; this leads to a reduction in the length of the chain axis from around 3 Å to around 2.8 Å due to the smaller size of Al. When compared to fluoborite, only alternate B-positions are occupied in painite; the remaining triangular tunnels are filled with Zr in trigonal prismatic co-ordination, leading to a tripling of the repeat distance along the chain-repeat direction. The hexagonal tunnels, empty in fluoborite, are occupied by [6]-co-ordinated Ca in painite. Thus from a bond-valence viewpoint, Zr and Ca must be regarded as framework cations in painite. In jeremejevite, the c-axis projection resembles that of fluoborite (Fig. 9a), but the character of the octahedral chains is different. The c dimension in jeremejevite is three times that of fluoborite, and every third octahedral site along c is empty; this empty site is bridged along the chain by a (BO_3) triangle.

In warwickite (Fig. 9b), the octahedral chains share edges to form ribbons four octahedra wide; these ribbons are canted at 60° to each other, and the triangular interstices are bridged by (BO_3) triangles. In ludwigite (Fig. 9c), the chains share edges to form zig-zag sheets with 5 octahedra on the zig and 3 octahedra on the zag. These sheets fit together such that there are triangular tunnels formed, across which the (BO_3) triangles fit. In projection, both hulsite (Fig. 9c) and pinakiolite are identical with regard to bond connectivity. They both consist of plane sheets of edge-sharing octahedra, separated by corrugated zig-zag sheets of edge-sharing octahedra with 3 octahedra on the zig and 3 octahedra on the zag. The interface between these two types of sheets forms triangular tunnels across which bridge the (BO_3) triangles. The difference between the two structures arises because of cation ordering over the large number of nonequivalent octahedral sites in each structure. In both hulsite and pinakiolite, the planar edge-sharing sheets consist of ordered arrangements of cations, (Sn,Fe^{3+}) and (Fe^{2+}, Mg) in hulsite, (Mn^{3+}) and (Mg,Mn) in pinakiolite. However, adjacent zig-zag sheets are equivalent in hulsite, whereas they are nonequivalent in pinakiolite, consisting alternately of (Mn^{3+}) and (Mg) octahedral sheets. In orthopinakiolite, there is one type of complex zig-

TABLE 4. $^{VI}M_x^{III}T_y\emptyset_z$ MINERALS BASED ON $[^{VI}M_z(T\emptyset_3)_y\emptyset_n]$ FRAMEWORKS

Mineral	Formula	a(Å)	b(Å)	c(Å)	β(°)	Sp.Gr.	Ref.
*Calcite	$[Ca(CO_3)]$	4.9896(2)	-	17.061(1)	-	$R\bar{3}c$	(1)
Gaspeite	$[Ni(CO_3)]$	4.598	-	14.723	-	$R\bar{3}c$	-
Magnesite	$[Mg(CO_3)]$	4.6328(2)	-	15.0129(5)	-	$R\bar{3}c$	(1)
Otavite	$[Cd(CO_3)]$	4.920	-	16.298	-	$R\bar{3}c$	-
Rhodochrosite	$[Mn^{2+}(CO_3)]$	4.7682(2)	-	15.6354(8)	-	$R\bar{3}c$	(1)
Siderite	$[Fe^{2+}(CO_3)]$	4.6916(4)	-	15.380(2)	-	$R\bar{3}c$	(1)
Smithsonite	$[Zn(CO_3)]$	4.6526(7)	-	15.026(2)	-	$R\bar{3}c$	(1)
Sphaerocobaltite	$[Co(CO_3)]$	4.658	-	14.958	-	$R\bar{3}c$	-
Ankerite	$[CaFe^{2+}(CO_3)]$	4.830(1)	-	16.167(3)	-	$R\bar{3}$	(2)
*Dolomite	$[CaMg(CO_3)_2]$	4.812(1)	-	16.020(3)	-	$R\bar{3}$	(1)
Kutnohorite	$[CaMn^{2+}(CO_3)_2]$	4.85	-	16.34	-	$R\bar{3}$	-
Minrecordite	$[CaZn(CO_3)_2]$	4.8183(4)	-	16.030(1)	-	$R\bar{3}$	-
Nordenskioldine	$[CaSn(BO_3)_2]$	4.853	-	15.920	-	$R\bar{3}$	-
Norsethite	$[BaMg(CO_3)_2]$	5.017(1)	-	16.77(1)	-	$R\bar{3}$	(3)
Jimboite	$[Mn_3(BO_3)_2]$	5.658(1)	8.740(1)	4.646(2)	-	Pnmn	(4)
*Kotoite	$[Mg_3(BO_3)_2]$	5.396(1)	8.297(2)	4.459(1)	-	Pnmn	(5)
Huntite	$[CaMg_3(CO_3)_4]$	9.5027(6)	-	7.8212(6)	-	R32	(6)
Fluoborite	$[Mg_3(BO_3)(F,OH)_3]$	8.827(3)	-	3.085(2)	-	$P6_3/m$	(7)
Painite	$CaZr[BAl_9O_{18}]$	8.715(2)	a	8.472(2)	-	$P6_3$	(8)
Jeremejevite	$[Al_6(BO_3)_5(OH)_3]$	8.56	-	8.18	-	$P6_3/m$	(9)
Warwickite	$[(Mg,Ti^{4+})_2(BO_3)O]$	9.197(7)	9.358(9)	3.085(2)	-	Pnam	(10)
Azoproite	$[Mg_2(Fe^{3+},Ti,Mg)(BO_3)O_2]$	9.26(1)	12.25(1)	3.01(1)	-	Pbam	-
Bonaccordite	$[Ni_2Fe^{3+}(BO_3)O_2]$	9.213(6)	12.229(7)	3.001(2)	-	Pbam	-
*Ludwigite	$[Mg_2Fe^{3+}(BO_3)O_2]$	9.14	12.45	3.05	-	Pbam	(11)
Vonsenite	$[Fe_2^{2+}Fe^{3+}(BO_3)O_2]$	9.463(1)	12.305(1)	3.073(1)	-	Pbam	(12)
Hulsite	$[(Fe^{2+},Mg)_2(Fe^{3+},Sn)(BO_3)O_2]$	10.695(4)	3.102(1)	5.431(1)	94.21(3)	P2/m	(13)
Pinakiolite	$[Mg_2Mn^{3+}(BO_3)O_2]$	21.79(1)	5.977(5)	5.341(5)	95.83(5)	C2/m	(10)
Orthopinakiolite	$[Mg_2Mn^{3+}(BO_3)O_2]$	18.357(4)	12.591(2)	6.068(1)	-	Pnnm	(14)
Takeuchiite	$[Mg_2Mn^{3+}(BO_3)O_2]$	27.50(1)	12.614(2)	6.046(1)	-	Pnnm	-
Wightmanite	$[Mg_5(BO_3)(OH)_5O]\cdot 2H_2O$	13.46(2)	3.102(5)	18.17(2)	91.60(5)	I2/m	(10)
Suanite	$[Mg_2B_2O_5]$	12.10(5)	3.12(2)	9.36(5)	104.3(5)	$P2_1/a$	(15)
Kurchatovite	$Ca[MgB_2O_5]$	36.292(8)	5.491(1)	11.120(2)		$Pc2_1b$	(16)
Sussexite	$[Mn_2^{2+}(B_2O_4OH)(OH)]$	12.77	10.70	3.25	-	$P2_1/a$	-
*Szaibelyite	$[Mg_2(B_2O_4OH)(OH)]$	12.577(2)	10.393(2)	3.139(1)	95.88(2)	$P2_1/a$	(17)
Hydromagnesite	$[Mg_5(CO_3)_4(OH)_2(H_2O)_4]$	10.105(5)	8.954(2)	8.378(4)	114.44(5)	$P2_1/c$	(18)
*Chalcomenite	$[Cu(SeO_3)(H_2O)_2]$	6.66	9.12	7.37	-	$P2_12_12_1$	(19)
Teineite	$[Cu(Te^{4+}O_3)(H_2O)_2]$	6.63	9.61	7.43	-	$P2_12_12_1$	(20)
*Ahlfeldite	$[Ni(SeO_3)(H_2O)_2]$	7.519	8.751	6.448	99.00	$P2_1/n$	-
Clinochalcomenite	$[Cu(SeO_3)(H_2O)_2]$	8.177	8.611	6.290	97.27	$P2_1/n$	-
Cobaltomenite	$[Co(SeO_3)(H_2O)_2]$	7.640	8.825	6.515	98.60	$P2_1/n$	-
Mandarinoite	$[Fe_2^{3+}(SeO_3)_3(H_2O)_3]\cdot 3H_2O$	16.810(4)	7.880(2)	10.019(2)	98.26(2)	$P2_1/c$	(21)
Trigonite	$Pb_3[Mn^{2+}(AsO_3)_2(AsO_2(OH))]$	7.26(2)	6.78(2)	11.09(2)	91.5(2)	Pn	(22)
Kinichilite	$[Fe_2^{2+}(Te^{4+}O_3)_3](Na,H)_2\cdot(H_2O)_n$	9.419	-	7.665	-	$P6_3/m$	-
*Zemannite	$[Zn_2^{2+}(Te^{4+}O_3)_3](Na,H)_2\cdot(H_2O)_n$	9.41(2)	-	7.64(2)	-	$P6_3/m$	(23)
Sonoraite	$[Fe_2^{3+}(Te^{4+}O_3)_2(OH)_2(H_2O)]\cdot H_2O$	10.984(2)	10.268(2)	7.917(2)	108.49(2)	$P2_1/c$	(24)
Emmonsite†	$[Fe_2^{3+}(Te^{4+}O_3)_3(H_2O)]\cdot H_2O$	7.90(1)	8.00(1)	7.62(1)	95.0(2)	$P\bar{1}$	(25)
Mackayite	$[Fe^{3+}(Te_2O_5)(OH)]$	11.80(1)	a	15.10(1)	-	$I4_1/acd$	(26)

Gaudefroyite	$Ca_4[Mn_3(BO_3)_3(CO_3)O_3]$	10.606(4)	a	5.879(1)	-	$P6_3$	(27)
Ferrotychite	$Na_6[Fe_2^{2+}(CO_3)_4](SO_4)$	13.962	-	-	-	Fd3	-
*Northupite	$Na_6[Mg_2(CO_3)_4]Cl$	14.069(2)	-	-	-	Fd3	(28)
Tychite	$Na_6[Mg_2(CO_3)_4](SO_4)$	13.90	-	-	-	Fd3	(29)
Sakhaite	$Ca_3[Mg(BO_3)_2](CO_3)(H_2O)_x$	14.690	-	-	-	F4,32	(30)
Schafarzikite	$[Fe^{2+}(Sb_2^{3+}O_4)]$	8.590(5)	-	5.913(5)	-	P4mbc	(31)
Trippkeite	$[Cu^{2+}(As_2^{3+}O_4)]$	8.592(4)	-	5.573(4)	-	P4mbc	(32)

References: (1) Effenberger et al. (1981); (2) Beran & Zemann (1977); (3) Lippman (1968); (4) Bondareva et al. (1978); (5) Effenberger & Pertlik (1984); (6) Dollase & Reeder (1986); (7) Dal Negro & Tadini (1974); (8) Moore & Araki (1976); (9) Rodellas et al. (1983); (10) Moore & Araki (1974); (11) Takéuchi et al. (1950); (12) Swinnea & Steinfink (1983); (13) Konnert et al. (1976); (14) Takéuchi et al., (1978); (15) Takéuchi (1952); (16) Yakubovich et al. (1976); (17) Takéuchi & Kudoh (1975); (18) Akao & Iwai (1977); (19) Gattow (1958); (20) Zemann & Zemann (1962); (21) Hawthorne (1984); (22) Pertlik (1978); (23) Matzat (1968); (24) Donnay et al. (1970); (25) Pertlik (1972); (26) Pertlik & Gieren (1977); (27) Yakubovich et al. (1975); (28) Dal Negro et al. (1975); (29) Watanabe (1933); (30) Chicagov et al. (1975); (31) Fischer & Pertlik (1975); Pertlik (1975).

† $\alpha = 96.7(2)$, $\gamma = 84.5(2)$.

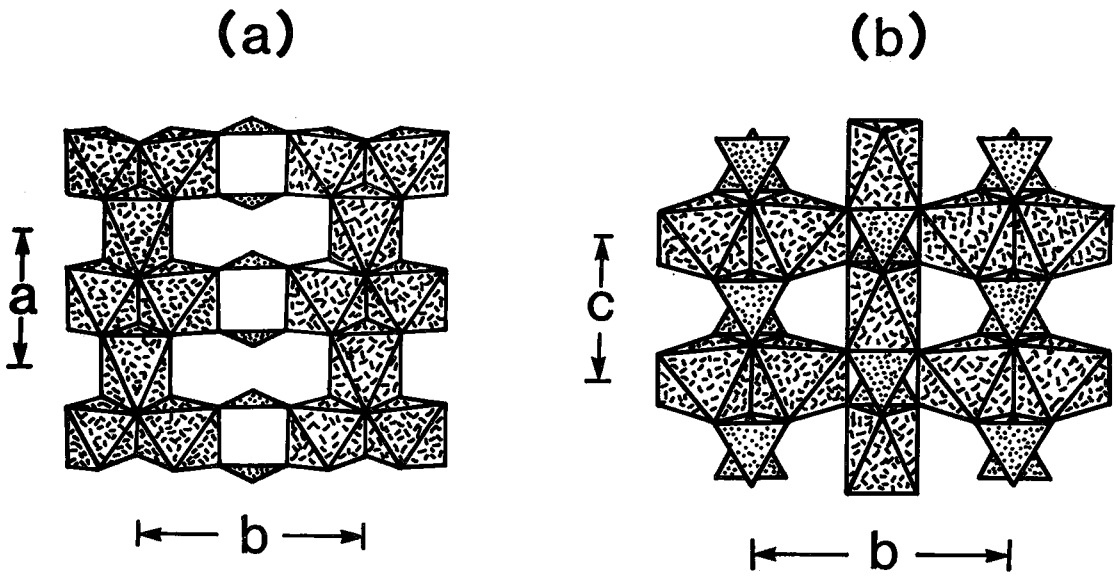

FIG. 7. The structure of the kotoite group of minerals: (a) projected down [001]; (b) projected down [100]. The structure module is of the form $[M_3(T\phi_3)_2]$, and there are no extra-module components.

zag sheet of edge-sharing octahedra, with the zig-zag sequence (7,3,3,3) consisting of a zig of 7 octahedra, followed by zag-zig-zag of 3 octahedra each. The sheets fit together (Fig. 9e) such that the (BO_3) triangles fit in the intersheet triangular tunnels. The structure of takeuchiite (Table 4) is presumably based on a variant of this pattern, with a different zig-zag arrangement. The most complex of these structures is wightmanite (Fig. 9f), in which 2×2 octahedral edge-sharing bundles and 1×2 octahedral edge-sharing ribbons link together, both by sharing octahedral vertices and by sharing vertices with (BO_3) triangles situated in the triangular tunnels of the structure. A very prominent feature of the framework is the presence of large channels running parallel to the edge-sharing octahedral chains (Fig. 9f);

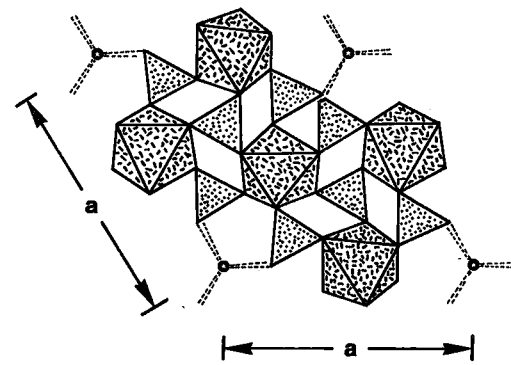

FIG. 8. The structure of huntite viewed down [001]; the star represent trigonal prismatically co-ordinated Ca.

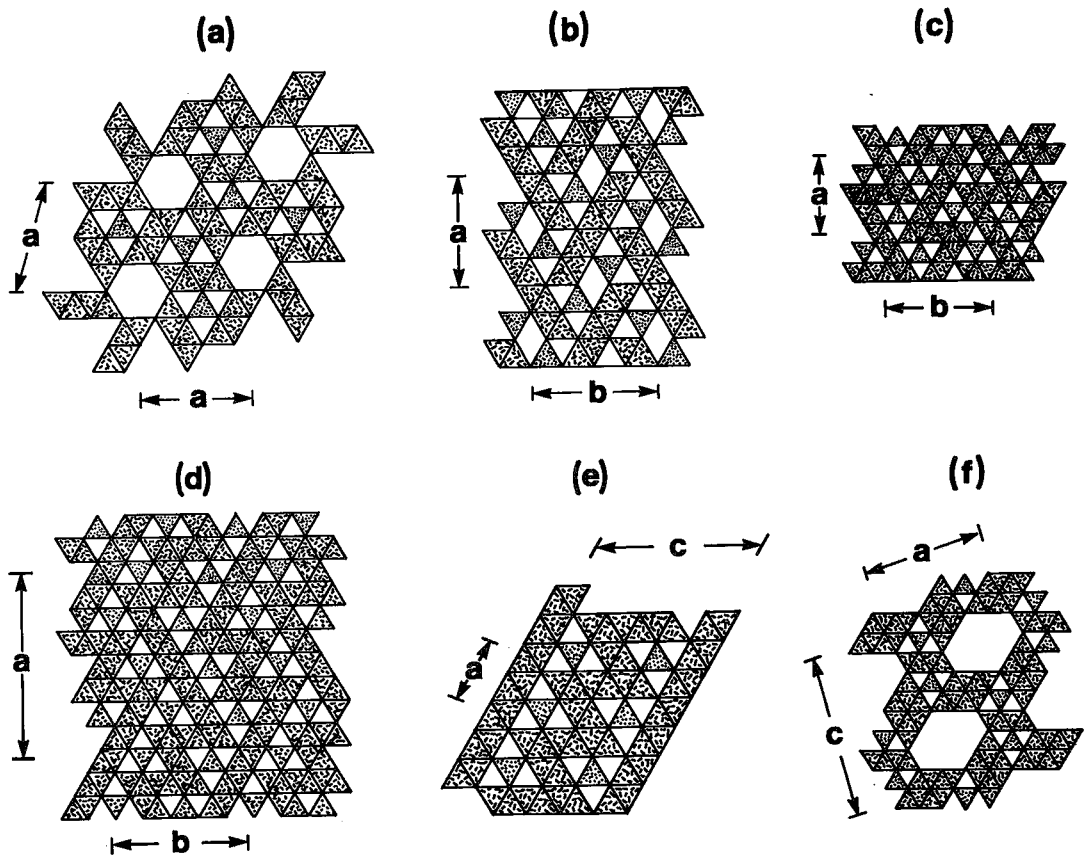

FIG. 9. The "3 Å wallpaper structures", shown as colorings of the 3^6 net: (a) $[M_3(T\phi_3)\phi_3]$, fluoborite type, orthogonal to the plane of the net; (b) $[M_2(T\phi_3)\phi]$, warwickite type; (c) $[M_3(T\phi_3)\phi_2]$, ludwigite type; (d) $[M_3(T\phi_3)\phi_2]$, orthopinakiolite type; (e) $[M_3(T\phi_3)\phi_2]$, hulsite type; (f) $[M_5(T\phi_3)\phi_6]$, wightmanite type. In all of these types, the framework stoichiometry can be modified by ordered vacancy substitutions along the length of the octahedral edge-sharing chains.

in character with their "drainpipe"-like aspect (Moore & Araki 1972), they are full of disordered (H_2O) molecules.

Although not noted by previous workers, some of the pyroborate minerals also belong to the "3 Å wallpaper structures". Perhaps the simplest framework is that of suanite (Fig. 10b); ribbons of edge-sharing octahedra are linked by corner-sharing with (B_2O_5) groups. The structure of the szaibelyite-group minerals (Fig. 10a) is considerably more complex. There are both single- and double-edge-sharing chains running parallel to the 3 Å axis. These link by sharing corners between the octahedral chains of both types, and by sharing corners with the (B_2O_5) pyroborate groups. This concludes the 3 Å "wallpaper" structures of Table 4.

The hydromagnesite structure (Fig. 11) has some "wallpaper" affinities, in that edge-sharing octahedral chains are also present in its structure. However, the structure does not map well on to a 3^6 net perpendicular to these chains, and its (simple) anion constitution is very different from the 3 Å minerals. Some adjacent chains share edges to form dimeric ribbons; these ribbons link through their vertices to form very corrugated sheets parallel to (100), with additional intrasheet linkage provided by (CO_3) groups subparallel to (100). There is also considerable intraframework linkage *via* hydrogen bonding from the (H_2O) group.

The minerals of the teineite group consist of distorted octahedra that link through sharing *trans* (H_2O) vertices to form ($M\phi_5$) chains parallel to [001], with (SeO_3) triangles bridging along the chains (Fig. 12a); note the analogy to the $[M_x(TO_4)_y\phi_n]$ 7 Å chain, sheet and framework structures (Moore 1970, 1975, Hawthorne 1985a, in prep.). The (SeO_3) groups also cross-link the chains to form a 3-dimensional framework (Fig. 12b). The ahlfeldite structures are thought to be a monoclinic distortion of the teineite-type arrangement.

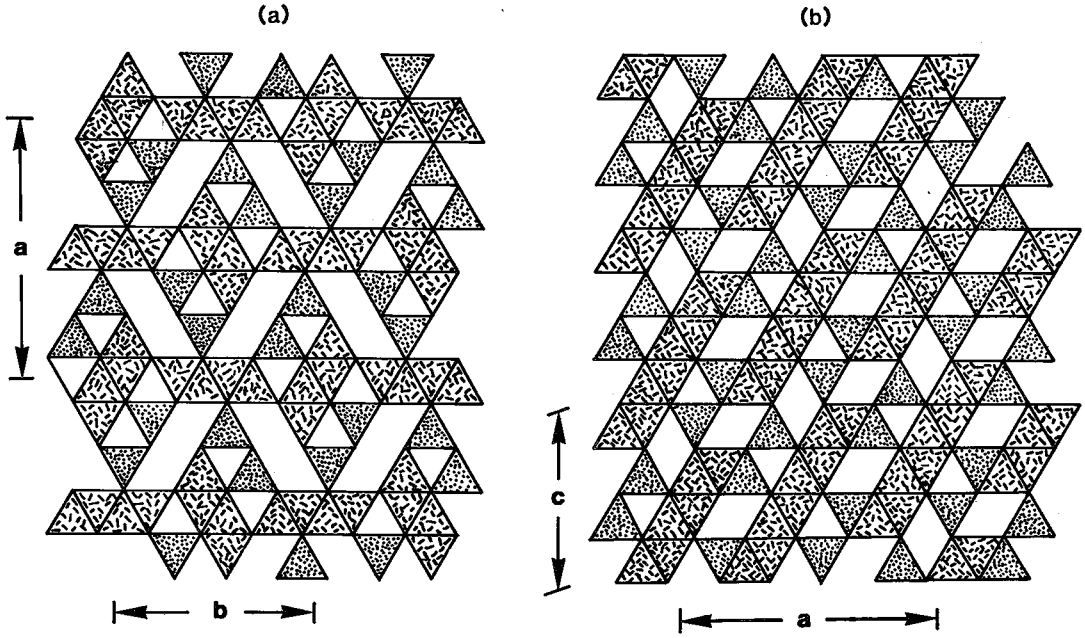

FIG. 10. The structure of the 3 Å pyroborate wallpaper minerals shown as idealized colorings of the 3^6 net: (a) $[M_2(T_2\phi_5)\phi]$ szaibelyite type; (b) $[M_2(T_2\phi_5)]$ suanite type.

Mandarinoite (Fig. 13a) is an elegant structure, a framework of corner-sharing octahedra and tetrahedra with an ordered arrangement of hydrogen-bonded (H_2O) molecules in the large interstices of the framework. Trigonite is also based on a framework of ($M\phi_6$) and ($T\phi_3$) groups in which the only linkage is corner-sharing between octahedra and tetrahedra (Fig. 13b). The module charge is balanced by the presence of Pb^{2+} as the extra-modular cation. Zemannite possesses a framework of the same stoichiometry as mandarinoite, but the linkage is more substantial. Face-sharing octahedral dimers link through corner-sharing with three (SeO_3) groups to form columns parallel to [001] (Fig. 14a). The (SeO_3) groups also cross-link to other columns to form the 3-dimensional framework (Fig. 14b), with extra-modular Na and (H_2O) disordered in the large channels. A third mineral with a similar stoichiometry of the framework is emmonsite. The structure is intermediate between that of mandarinoite and zemannite, with edge-sharing ($Fe^{3+}_2\phi_{10}$) dimers linked by corner-sharing with (TeO_3) groups to form a fairly open framework.

Sonoraite has a framework with prominent octahedral chains parallel to [101]. The octahedra alternately share edges and corners (Fig. 15a) and are cross-linked into a framework by (TeO_3) groups. Mackayite has a somewhat different framework (Fig. 15b). Pairs of (TeO_3) groups link to form (Te_2O_5) dimers, and pairs of ($Fe\phi_6$) octahedra share edges to form ($Fe_2\phi_{10}$) dimers; the dimers then link corners in three dimensions to form a framework. Gaudefroyite (Fig. 16a,b) consists of edge-sharing chains of octahedra and *en échelon* triangles running parallel to [001]; the triangles link to adjacent chains to form a very open 3-dimensional framework. Extra-modular Ca occupies the large channels in this framework, balancing the module charge. Lastly, the

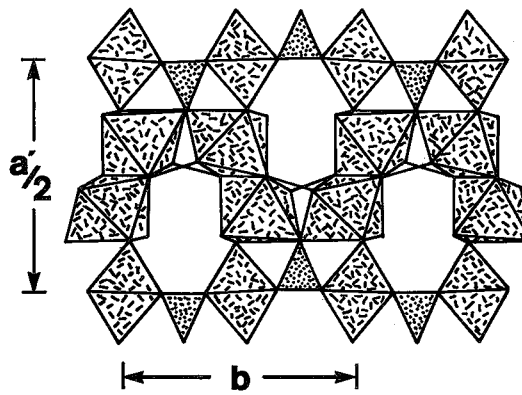

FIG. 11. The structure of hydromagnesite viewed down [001]; in the central convolute chain of octahedra running parallel to [010], note that some of the ($T\phi_3$) groups are seen 'edge-on' and appear only as lines connecting neighboring octahedra.

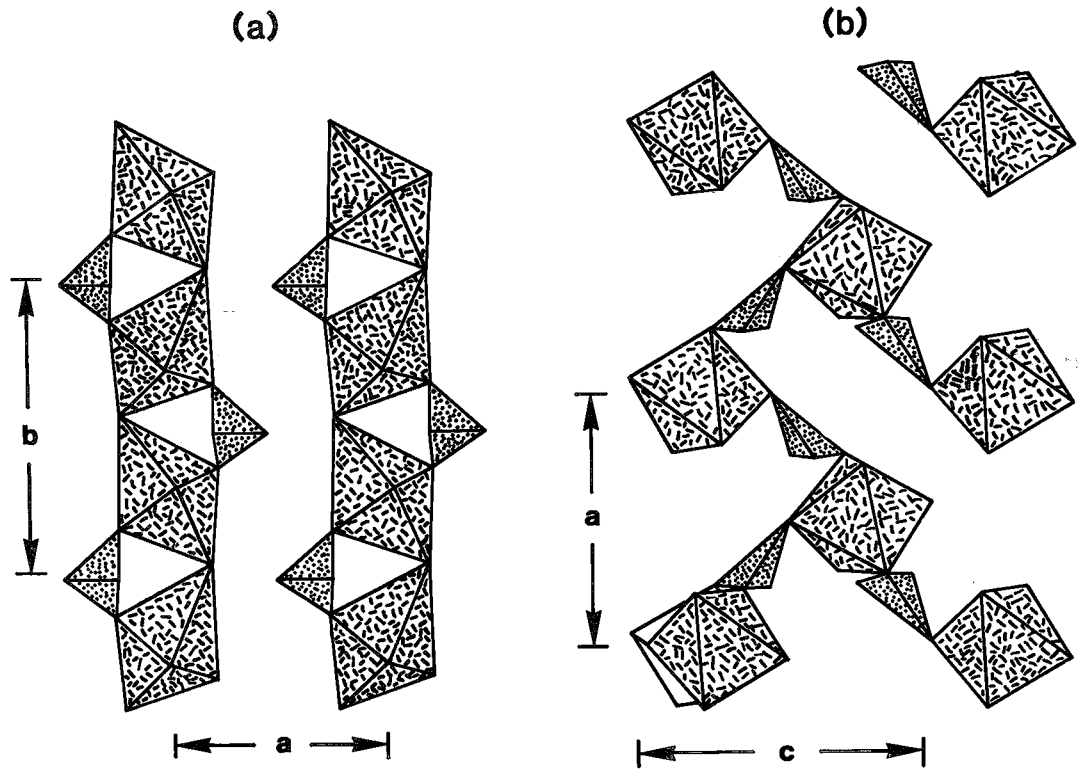

FIG. 12. The structure of teineite: (a) projected down [001]; (b) projected down [010]. Note that the ($Te\phi_3$) groups are pyramidal rather than planar [as for (CO_3) and (BO_3) groups], and hence are shown as tetrahedra rather than as triangles; however, the connectivity of these groups is topologically the same as for the planar triangular groups.

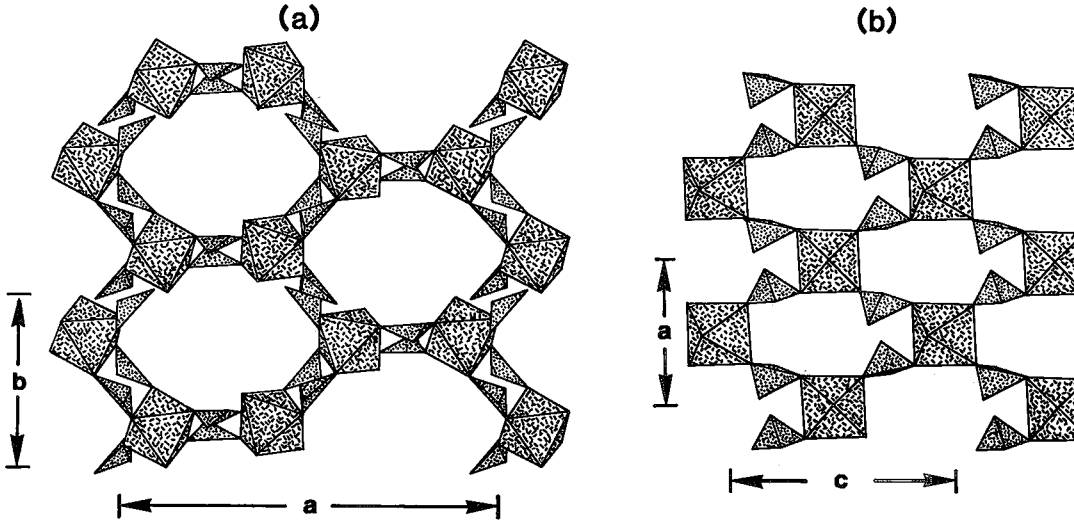

FIG. 13. The framework modules of (a) mandarinoite, projected down [001]; (b) trigonite, projected down [010]. The large cavities in mandarinoite are filled with an ordered arrangement of (H_2O) groups.

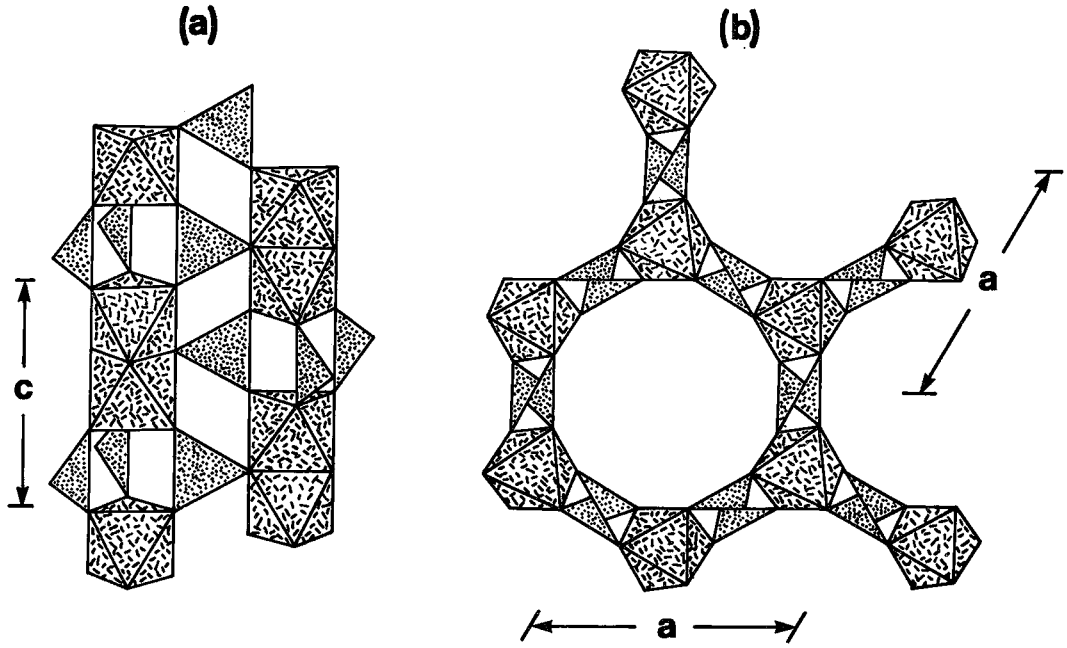

FIG. 14. The framework module of zemannite (a) projected along [110]; (b) projected down [001]. The large channels are filled with extra-modular Na (not shown) and (H_2O) groups.

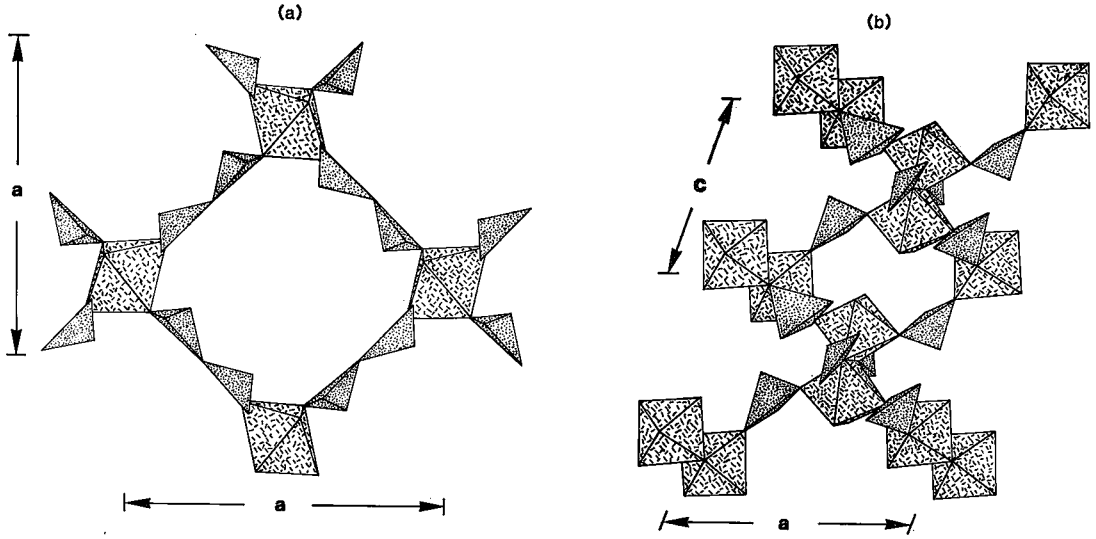

FIG. 15. The framework modules in (a) mackayite, projected down [001]; (b) sonoraite, projected down [010].

minerals of the trippkeite group (Fig. 16c) consist of edge-sharing chains of octahedra and corner-sharing chains of triangles, both running parallel to [001] and linking by corner-sharing to form a dense framework.

STRUCTURAL TRENDS

Hawthorne (1985a,b) has shown how the idea of fundamental building blocks and structure modules can be used in conjunction with the structure-based

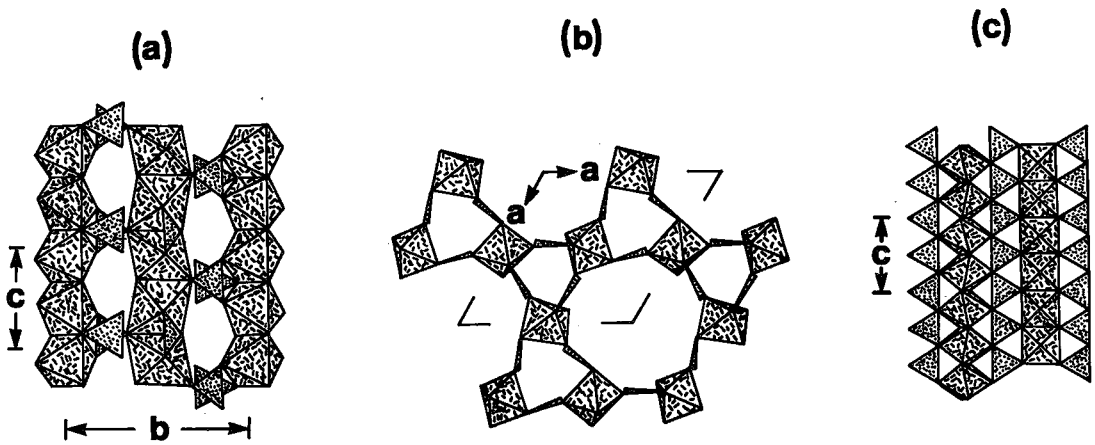

FIG. 16. The structures of (a) gaudefroyite, projected down [110]; (b) gaudefroyite, projected down [001]; (c) tripp-keite, projected down [110].

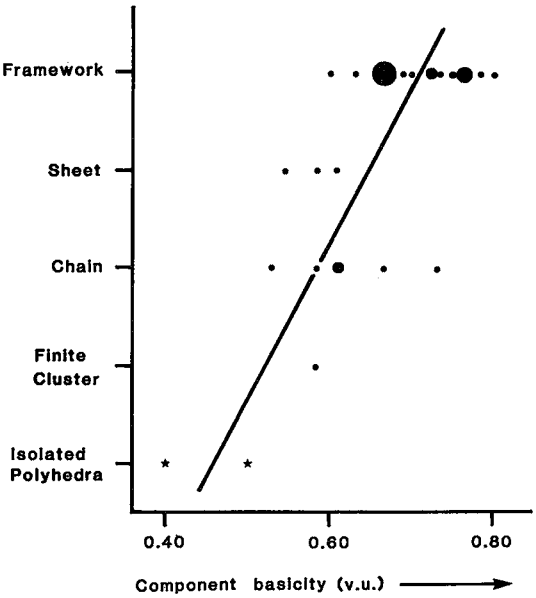

FIG. 17. Structure type as a function of the Lewis basicity of the component oxyanions $[(M\phi_6) + (T\phi_6)]$; the size of the symbols is proportional to the number of minerals with that particular basicity and structure type. The stars represent synthetic compounds.

scale of Lewis acid and base strengths developed by Brown (1981), to provide some insight into structure type as a function of chemical composition. The Lewis acid strength of a cation is defined as the cation valence divided by the average cation co-ordination number; it is thus the average valence of a bond formed by that cation. Of course, in individual structures there is considerable dispersion about this value for individual bonds. The Lewis base strength of an anion is the average bond-valence of a bond formed by that anion, be it a simple or a complex anion.

The hypothesis of Hawthorne (1983) considers the polymerization of the more tightly bonded oxyanions in the structure. Increasing polymerization will decrease the Lewis base strength of the linked oxyanions, suggesting that the degree of polymerization in these structures should be related to the average Lewis base strength of their component oxyanions (*i.e.*, $[(M\phi_6)_x + (T\phi_3)_y]$). Hawthorne (1985a) showed this to be the case for the $[^{VI}M(^{IV}T\phi_4)_2\phi_n]$ minerals, and Figure 17 shows this to be the case for the $[^{VI}M_x(^{III}T\phi_3)_y\phi_n]$ structures considered here. There is considerable scatter in the data, but this is to be expected. The division into the different classes is a very coarse one; there is considerable variation of the degree of polymerization of the component oxyanions within any one class, and overlap between classes will also occur. In addition, one would expect the pH of the environment of crystallization to affect the polymerization of the FBBs. Consequently, the general correlation of Figure 17 suggests that this approach is worth pursuing, both with regard to understanding the general structural trends in these groups and with regard to the correlation of structure with paragenesis.

INTERMODULE LINKAGE AND EXTRA-MODULE CATIONS

The valence-matching principle (Brown 1981) states that the most stable structures will form when the Lewis acid strength of the cation is closest to the Lewis base strength of the anion. Hawthorne (1985a)

has exploited this rule by considering the principal module of a structure as a very complex (oxy)anion, and relating the Lewis basicity of the module *via* the valence-matching principle to the Lewis acidity of the extra-modular cations of the structure. Thus the characteristics of the extra-modular cations can be rationalized or even predicted on this basis, and the scheme works fairly well for tetrahedral–octahedral minerals of $MT_2\phi_n$ stoichiometry.

Calculation of module basicity hinges on the use of the most appropriate co-ordination number of the anion. Hawthorne (1985a) used an oxygen co-ordination number of [4], except where O^{2-} is bonded to M^{3+} and T^{6+}, where a co-ordination number of [3] was used. A different procedure is used here. Many investigators have commented on the fact that the bond lengths or bond valences around a single cation in a structure tend to be as similar as possible, and Brown (1977) has used this observation (for both cations and anions) to successfully predict bond lengths in structures, given the initial bond-connectivity. Here I will consider the optimum arrangement to be that which gives the most nearly equal bond-valences from the extra-modular cation to the structure module. In some cases, an equal distribution of bond valences is forced by the structure arrangement, no matter what co-ordination numbers are assigned to the anion. Using the above criteria, one might expect these minerals to be particularly accommodating with regard to variations in the chemistry of the extra-modular cation.

Finite-cluster structures

In the baylissite module (Fig. 1), there are three types of simple anion: there are four oxygen atoms bonded just to C, receiving 1.333 v.u. and requiring a further 0.667 v.u.; there are two oxygen atoms bonded to C and Mg, receiving 1.667 v.u. and requiring a further 0.333 v.u.; there are four oxygen atoms bonded to one Mg and 2H, each receiving 2.333 v.u. and forming two hydrogen bonds of strength 0.167 v.u. If the hydrogen bonds are assigned to the oxygen atoms just bonded to C, bond valences from the extra-modular cations may be calculated for a variety of simple anion co-ordination numbers. The Lewis acidity of the extra-modular cations may be assigned from that combination of anion co-ordination numbers that gives the most uniform set of extra-module bond-valences. The results of these calculations for baylissite are shown in Table 5. The most uniform set of bond valences is for the combination of co-ordination numbers [3] and [4], forecasting a [6]-co-ordinated monovalent extra-modular cation or a [12]-co-ordinated divalent cation; in baylissite, the extra-modular cation is K, with a co-ordination number of [5] or [7], in good agreement with the calculations. The optimum basicity of the

TABLE 5. ANION CO-ORDINATION NUMBERS, BOND-VALENCES AND PREDICTED EXTRA-MODULE CATION CO-ORDINATION NUMBERS

C.N.	bv(1)	bv(2)	<bv>	$[]^+$	$[]^{2+}$	$[]^{3+}$
			Baylissite			
3	0.17	0.33	0.20	5	10	15
4	0.11	0.16	0.13	8	16	-
5	0.08	0.11	0.09	11	22	-
3,4	0.17	0.17	0.17	6	12	18
			Sahamalite-type			
3	0.33	0.33	0.33	3	6	9
4	0.22	0.17	0.20	5	10	15
5	0.17	0.11	0.14	7	14	21
			Dunasite-type			
3	0.33	0.17	0.25	4	8	12
4	0.22	0.08	0.14	7	14	21
3,4	0.22	0.17	0.20	5	10	15
3,5	0.17	0.17	0.17	6	12	18
			Chalconatronite-type			
3	0.25	0.33	0.29	3	7	10
4	0.17	0.17	0.17	6	12	18
			Eitelite-type			
3	0.33	-	0.33	3	6	9
4	0.17	-	0.17	6	12	18
5	0.11	-	0.11	9	18	-
			Tunisite			
3	0.17	0.33	0.25	4	8	12
4	0.08	0.22	0.14	7	14	21
3,4	0.17	0.22	0.20	5	10	15
3,5	0.17	0.17	0.17	6	12	18
			Denningite			
3	0.33	0.33	0.33	3	6	9
4	0.17	0.22	0.20	5	10	15
3,4	0.33	0.22	0.28	4	7	11
			Trigonite			
3	0.67	-	0.67	1	3	4
4	0.33	-	0.33	3	6	9
5	0.22	-	0.22	4	9	13
			Gaudefroyite			
4	0.25	0.50	0.38	3	5	8
5	0.17	0.33	0.25	4	8	12
6	0.13	0.25	0.19	5	11	16
4,6	0.25	0.25	0.25	4	8	12
			Northupite			
3	0.33	-	0.33	3	6	9
4	0.17	-	0.17	6	12	-
5	0.11	-	0.11	9	-	-
			Sakhaite			
3	0.67	-	0.67	2	3	5
4	0.33	-	0.33	3	6	9
5	0.22	-	0.22	5	9	14

C.N.: assumed anion co-ordination numbers; bv(1): bond valence (v.u.) required to satisfy one type of oxygen in the structure, for the assumed anion C.N.; bv(2): bond valence required to satisfy the other type of oxygen in the structure; <bv>: mean bond-valence to structure module from the extra-module cations (= module basicity); []: predicted co-ordination number for monovalent (+), divalent (2+) and trivalent (3+) extra-module cations.

module is 0.17 v.u., and Na would be the ideal extra-modular cation, but the solution for [4]-co-ordination anions is also fairly reasonable, giving a module basicity of 0.13 v.u., which would favor K as an extra-modular cation, as observed in baylissite.

Finite-chain structures

The results for the chain structures with extra-modular cations are given in Table 5. For sahamalite, the most even distribution of bond valences occurs for an anion co-ordination number of [3]. This would lead to [3]-co-ordinated monovalent cations, [6]-co-ordinated divalent cations and [9]-co-ordinated trivalent cations; in sahamalite, the extra-modular cation is [9]-co-ordinated *REE,* in good agreement with the calculation.

The dundasite-type chain is a good test of this method, as there are several different minerals with this structure module. The optimum bond-valence distribution occurs for the combination of anion co-ordination numbers [3] and [5], which predicts a [6]-co-ordinated monovalent or [12]-co-ordinated divalent extra-modular cation. The extra-modular cation in hydrodresserite is Ba, with an effective co-ordination number of [12] (co-ordination = $6O^{2-}$ + $3H_2O$ = (6×1) + (3×2) = 12 bonds to the structure module) in agreement with the prediction. The extra-modular cation in dawsonite is [6]-co-ordinated Na, again in agreement with predictions. The next closest solution is for anion co-ordination numbers of [3] and [4], which predicts [5]-co-ordinated monovalent or [10]-co-ordinated divalent extra-modular cations; this is in good agreement with the [10]-co-ordinated Pb, Ba and Sr found in the minerals of the dundasite group.

For chalconatronite, the optimum bond-valence distribution is for an anion co-ordination number of [4], which predicts a [6]-co-ordinated monovalent or [12]-co-ordinated divalent extra-modular cation. Chalconatronite has [6]-co-ordinated Na as the extra-modular cation, in agreement with the prediction.

Infinite-sheet structures

Calculations for the infinite-sheet structures (with extra-modular cations) are given in Table 5. For the eitelite group of minerals, there is only one type of simple anion in the structure module, and thus the bond-valence distributions of any extra-modular cation will always be optimum. For [3]-co-ordinated anions, a co-ordination of [3] for a monovalent cation and a co-ordination of [6] for a divalent cation are predicted. In the divalent case, this would actually form a framework to give a calcite-structure module. For [4]-co-ordinated anions, the module basicity is 0.17, giving a co-ordination number of [6] for an extra-modular monovalent cation, and suggesting Na as the optimum cation. For [5]-co-ordinated anions, K is predicted for the extra-modular cation, with a co-ordination number of [9]. In eitelite, the extra-modular cation is [6]-co-ordinated Na, in buetschliite, the extra-modular cation is [9]-co-ordinated K, both in agreement with the predictions.

In tunisite, optimum bond-valence distribution occurs for simple anion co-ordination numbers of [3] and [5], with [3] and [4] also giving reasonable values; tunisite contains [5]-co-ordinated Na and [10]-co-ordinated Ca as extra-modular cations, in agreement with the predicted co-ordinations in Table 5. For denningite, optimum bond-valence distribution would predict [6]-co-ordinated divalent or [9]-co-ordinated trivalent extra-modular cations; [8]-co-ordinated (Ca,Mn) occurs.

Infinite-framework structures

Most of the infinite framework structures have neutral structure-modules and no extra-modular cations; calculations for the few frameworks with extra-modular cations are given in Table 5.

For trigonite, the bond-valence distribution is always uniform and a wide variety of extra-modular cations could occur. Pb is actually observed, with co-ordinations of [4+3] (4 short and 3 long bonds), [3+2], and [3+2]. These are low co-ordination numbers for Pb, but they are compatible with the basicity of the framework module, and the stereoactive lone-pair effect in Pb allows these low co-ordinations to be realized. For gaudefroyite, the optimum bond-valence arrangement predicts extra-modular cation co-ordinations of [4] for monovalent cations and [8] for divalent cations; gaudefroyite has [7]- and [9]-co-ordinated Ca, in good agreement with prediction.

Summary

Minerals may be ordered into structural hierarchies according to the polymerization of those cation co-ordination polyhedra of higher bond-valences. This hypothesis has been applied to a diverse group of carbonates, triangular borates, selenites, tellurites, arsenites and antimonites containing octahedrally co-ordinated cations. The mode of polymerization of the fundamental building block of a structure is related to the Lewis basicity of the simple oxyanions that constitute the cluster. If the structure module is treated as a very complex oxyanion, the Lewis basicity of the module may be related to the Lewis acidity of the extra-modular cations for a variety of co-ordination numbers of simple anions; with the constraint that the preferred co-ordination numbers of simple anions result in the least dispersion in bond valences of the extra-modular cations, the identity and co-ordination number of the extra-modular cation can be predicted with fair success.

ACKNOWLEDGEMENTS

Financial support for this work was provided by the Natural Sciences and Engineering Research Council of Canada in the form of a fellowship and an operating grant to the author.

REFERENCES

AKAO, M. & IWAI, S. (1977): The hydrogen bonding of artinite. *Acta Cryst.* **B33**, 3951-3953.

BERAN, A. & ZEMANN, J. (1977): Refinement and comparison of the crystal structures of a dolomite and of an Fe-rich ankerite. *Tschermaks Mineral. Petrog. Mitt.* **24**, 279-286.

BONDAREVA, O.S., SIMENOV, M.A. & BELOV, N.V. (1978): The crystal structure of synthetic jimboite $Mn_3(BO_3)_2$. *Sov. Phys. Cryst.* **23**, 82-83.

BROWN, I.D. (1977): Predicting bond lengths in inorganic crystals. *Acta Cryst.* **B33**, 1305-1310.

_____ (1981): The bond-valence method: an empirical approach to chemical structure and bonding. *In* Structure and Bonding in Crystals II (M. O'Keeffe & A. Navrotsky, eds.). Academic Press, New York.

BUCAT, R.B., PATRICK, J.M., WHITE, A.H. & WILLIS, A.C. (1977): Crystal structure of baylissite, $K_2Mg(CO_3)_2 \cdot 4H_2O$. *Aust. J. Chem.* **30**, 1379-1382.

CHICAGOV, A.V., SIMONOV, M.A. & BELOV, N.V. (1975): Crystal structure of sakhaite $Ca_3Mg(BO_3)_2CO_3 \cdot xH_2O$. *Sov. Phys. Dokl.* **19**, 559-561.

COCCO, G., FANFANI, L., NUNZI, A. & ZANAZZI, P.F. (1972): The crystal structure of dundasite. *Mineral. Mag.* **38**, 564-569.

CORAZZA, E., SABELLI, C. & VANNUCCI, S. (1977): Dawsonite: new mineralogical data and structure refinement. *Neues Jahrb. Mineral. Monatsh.*, 381-397.

DAL NEGRO, A., GIUSEPPETTI, G. & TADINI, C. (1975): Refinement of the crystal structure of northupite: $Na_3Mg(CO_3)_2Cl$. *Tschermaks Mineral. Petrog. Mitt.* **22**, 158-163.

_____ & TADINI, C. (1974): Refinement of the crystal structure of fluoborite, $Mg_3(F,OH)_3(BO_3)$. *Tschermaks Mineral. Petrog. Mitt.* **21**, 94-100.

DOLLASE, W.A. & REEDER, R.J. (1986): Crystal structure refinement of huntite, $CaMg_3(CO_3)_4$, with X-ray powder data. *Amer. Mineral.* **71**, 163-166.

DONNAY, G., STEWART, J.M. & PRESTON, H. (1970): The crystal structure of sonoraite, $Fe^{3+}Te^{4+}O_3(OH) \cdot H_2O$. *Tschermaks Mineral. Petrog. Mitt.* **14**, 27-44.

DUSAUSOY, Y. & PROTAS, J. (1969): Détermination et étude de la structure cristalline de la rodalquilarite, chlorotellurite acide de fer. *Acta Cryst.* **B25**, 1551-1558.

EFFENBERGER, H., KLUGER, F., PERTLIK, F. & ZEMANN, J. (1981): Tunisit: Kristallstruktur und Revision der chemischem Formel. *Tschermaks Mineral. Petrog. Mitt.* **28**, 65-77.

_____ & PERTLIK, F. (1984): Verfeinerung der Kristallstrukturen der isotypen Verbindungen $M_3(BO_3)_2$ mit M = Mg, Co und Ni (Strukturtyp: Kotoit). *Z. Krist.* **166**, 129-140.

FISCHER, R. & PERTLIK, F. (1975): Verfeinerung der Kristallstruktur des Schafarzikits, $FeSb_2O_4$. *Tschermaks Mineral. Petrog. Mitt.* **22**, 236-241.

GATTOW, G. (1958): Die Kristallstruktur von $CuSeO_3 \cdot 2H_2O$ (Chalkomenit). *Acta Cryst.* **11**, 377-383.

HAIR, N.J. & BEATTIE, J.K. (1977): Structure of Hexaaquairon (III) nitrate trihydrate. Comparison of iron (II) and iron (III) bond lengths in high-spin octahedral environments. *Inorg. Chem.* **16**, 245-250.

HAWTHORNE, F.C. (1983): Graphical enumeration of polyhedral clusters. *Acta Cryst.* **A39**, 724-736.

_____ (1984): The crystal structure of mandarinoite, $Fe^{3+}_2Se_3O_9 \cdot 6H_2O$. *Can. Mineral.* **22**, 475-480.

_____ (1985a): Towards a structural classification of minerals: the $^{VI}M^{IV}T_2\phi_n$ minerals. *Amer. Mineral.* **70**, 455-473.

_____ (1985b): Modular crystallography: an approach to the structural classification of minerals. 9th European Crystallography Meeting, Torino, Italy (abstr.).

_____ (1985c): Refinement of the crystal structure of bloedite: structural similarities in the $[^{VI}M(^{IV}T\phi_4)_2\phi_n]$ finite-cluster minerals. *Can. Mineral.* **21**, 669-674.

_____ & EBY, R.K. (1985): Refinement of the crystal structure of lindgrenite. *Neues Jahrb. Mineral. Monatsh.*, 234-240.

KONNERT, J.A., APPLEMAN, D.E., CLARK, J.R., FINGER, L.W., KATO, T. & MIURA, Y. (1976): Crystal structure and cation distribution of hulsite, a tin-iron borate. *Amer. Mineral.* **61**, 116-122.

LIMA-DE-FARIA, J. (1983): A proposal for a structural classification of minerals. *Garcia de Orta, Ser. Geol., Lisboa,* **6**, 1-14.

LIPPMANN, F. (1968): Die Kristallstruktur des Norsethit, $BaMg(CO_3)_2$. *Tschermaks Mineral. Petrog. Mitt.* **12**, 299-318.

MATZAT, E. (1968): Die Kristallstruktur eines unbenannten zeolithartigen Telluritminerals, $\{(Zn,Fe)_2[TeO_3]_3\}Na_xH_2 \cdot yH_2O$. *Tschermaks Mineral. Petrog. Mitt.* **12**, 108-117.

MOORE, P.B. (1970): Structural hierarchies among minerals containing octahedrally coordinating oxygen. I. Stereoisomerism among corner-sharing octahedral and tetrahedral chains. *Neues Jahrb. Mineral. Monatsh.*, 163-173.

_____ (1975): Laueite, pseudolaueite, stewartite and metavauxite: a study in combinatorial polymorphism. *Neues Jahrb. Mineral. Abh.* **123**, 148-159.

_____ & ARAKI, T. (1972): Wightmanite, $Mg_5(O)(OH)_5[BO_3] \cdot nH_2O$, a natural drainpipe. *Nature Phys. Sci.* **239**, 25-26.

_____ & _____ (1974): Pinakiolite, $Mg_2Mn^{3+}O_2[BO_3]$; warwickite, $Mg(Mg_{0.5}Ti_{0.5})O[BO_3]$; wightmanite, $Mg_5(O)(OH)_5[BO_3] \cdot nH_2O$: crystal chemistry of complex 3 Å wallpaper structures. *Amer. Mineral.* **59**, 985-1004.

_____ & _____ (1976): Painite, $CaZrB[Al_9O_{18}]$: its crystal structure and relation to jeremejevite, $B_5[\square_3Al_6(OH)_3O_{15}]$, and fluoborite, $B_3[Mg_9(F,OH)_9O_9]$. *Amer. Mineral.* **61**, 88-94.

_____ & _____ (1977): Mitridatite, $Ca_6(H_2O)_6[Fe^{III}_9O_6(PO_4)_9] \cdot 3H_2O$. A noteworthy octahedral sheet structure. *Inorg. Chem.* **16**, 1096-1106.

MOSSET, A., BONNET, J.-J. & GALY, J. (1978): Structure cristalline de la chalconatronite synthétique: $Na_2Cu(CO_3)_2 \cdot 3H_2O$. *Z. Krist.* **148**, 165-177.

PABST, A. (1973): The crystallography and structure of eitelite, $Na_2Mg(CO_3)_2$. *Amer. Mineral.* **58**, 211-217.

_____ (1974): Synthesis, properties and structure of $K_2Ca(CO_3)_2$, buetschliite. *Amer. Mineral.* **59**, 353-358.

PAULING, L. (1960): *The Nature of the Chemical Bond* (3rd edition). Cornell University Press, Ithaca, New York.

PERTLIK, F. (1972): Der Strukturtyp von Emmonsit, $\{Fe_2[TeO_3]_3 \cdot H_2O\} \cdot xH_2O$ ($x = 0$–1). *Tschermaks Mineral. Petrog. Mitt.* **18**, 157-168.

_____ (1975): Verfeinerung der Kristallstruktur von synthetischem Trippkeit, $CuAs_2O_4$. *Tschermaks Mineral. Petrog. Mitt.* **22**, 211-217.

_____ (1978): The crystal structure of trigonite, $Pb_3Mn(AsO_3)_2(AsO_2OH)$. *Tschermaks Mineral. Petrog. Mitt.* **25**, 95-105.

_____ & GIEREN, A. (1977): Verfeinerung der Kristallstruktur von Mackayit, $Fe(OH)[Te_2O_5]$. *Neues Jahrb. Mineral. Monatsh.*, 145-154.

_____ & PREISINGER, A. (1983): Crystal structure of sahamalite $(Mg,Fe)RE_2(CO_3)_4$. *Tschermaks Mineral. Petrog. Mitt.* **31**, 39-46.

RIBÁR, B., PETROVIĆ, D., DJURIĆ, S. & KRSTANOVIĆ, I. (1976): The crystal structure of hexaquomanganese nitrate, $Mn(OH_2)_6(NO_3)_2$. *Z. Krist.* **144**, 334-340.

RODELLAS, C., GARCÍA-BLANCO, S. & VEGAS, A. (1983): Crystal structure refinement of jeremejevite ($Al_6B_5F_3O_{15}$). *Z. Krist.* **165**, 255-260.

STEPHAN, G.W. & MACGILLAVRY, C.H. (1972): The crystal structure of nesquehonite, $MgCO_3 \cdot 3H_2O$. *Acta Cryst.* **B28**, 1031-1033.

SWINNEA, J.S. & STEINFINK, H. (1983): Crystal structure and Mössbauer spectrum of vonsenite, $2FeO \cdot FeBO_3$. *Amer. Mineral.* **68**, 827-832.

SZYMAŃSKI, J.T. (1982): The crystal structure of hydrodresserite, $BaAl_2(CO_3)_2(OH)_4 \cdot 3H_2O$. *Can. Mineral.* **20**, 253-262.

TAKÉUCHI, Y. (1952): The crystal structure of magnesium pyroborate. *Acta Cryst.* **5**, 574-581.

_____, HAGA, N., KATO, T. & MIURA, Y. (1978): Orthopinakiolite, $Me_{2.95}O_2[BO_3]$: its crystal structure and relationship to pinakiolite, $Me_{2.90}O_2[BO_3]$. *Can. Mineral.* **16**, 475-485.

_____ & KUDOH, Y. (1975): Szaibelyite, $Mg_2(OH)[B_2O_4(OH)]$: crystal structure, pseudosymmetry, and polymorphism. *Amer. Mineral.* **60**, 273-279.

_____, WATANABE, T. & ITO, T. (1950): The crystal structure of warwickite, ludwigite and pinakiolite. *Acta Cryst.* **3**, 98-107.

WALITZI, E.M. (1965): Die Kristallstruktur von Denningit, $(Mn,Ca,Zn)Te_2O_5$. Ein Beispiel für die Koordination um vierwertiges Tellur. *Tschermaks Mineral. Petrog. Mitt.* **10**, 241-255.

WATANABÉ, T. (1933): Les structures cristallines de la northupite $2MgCO_3 \cdot 2Na_2CO_3 \cdot 2NaCl$ et de la tychite $2MgCO_3 \cdot Na_2SO_4 \cdot 2Na_2CO_3$. *Sci. Papers Phys. Chem. Res. (Tokyo)* **21**, 40-62.

YAKUBOVICH, O.V., SIMENOV, M.A., BELOKONEVA, E.L., EGOROV-TISMENKO, YU. K. & BELOV, N.V. (1976): Crystalline structure of Ca,Mg-diorthotriborate (pyroborate) kurchatovite $CaMg(B_2O_5)$. *Sov. Phys. Cryst.* **21**. 542-544.

_____, _____ & BELOV, N.V. (1975): Structure refinement for gaudefroyite. *Sov. Phys. Cryst.* **20**, 87-88.

ZEMANN, A. & ZEMANN, J. (1962): Die Kristallstruktur von Teineit. Ein Beispiel für die Korrektur einer chemischen Formel auf Grund der Strukturbestimmung. *Acta Cryst.* **15**, 698-702.

Received June 27, 1985, revised manuscript accepted May 26, 1986.